UCLA
UCLA Previously Published Works

Title

An assessment of the temporal variability in the annual cycle of daily Antarctic sea ice in the NCAR Community Earth System Model, Version 2: A comparison of the historical runs with observations

Permalink

https://escholarship.org/uc/item/8v34h1b5

Authors

Raphael, Marilyn
Handcock, Mark S
Holland, Marika M
et al.

Publication Date

2020-06-10

DOI

10.1002/essoar.10503305.1

Peer reviewed

eScholarship.org Powered by the California Digital Library
University of California

An assessment of the temporal variability in the annual cycle of daily Antarctic sea ice in the NCAR Community Earth System Model, Version 2: A comparison of the historical runs with observations

Marilyn N. Raphael[1], Mark S. Handcock[1], Marika M. Holland[2], Laura L. Landrum[2]

[1]University of California, Los Angeles
[2]National Center for Atmospheric Research

Key Points:

- Antarctic sea ice extent variability is dominated by sub-decadal variability and that is well represented in the CESM2 simulations.
- The CESM2 simulates an annual cycle of sea ice extent that is comparable in size to that observed but begins its advance and retreat later.
- The later retreat of the CESM2 sea ice is potentially related to its simulation of the semi-annual oscillation of the circumpolar trough.

Corresponding author: Marilyn N. Raphael, `raphael@geog.ucla.edu`

Abstract

Understanding the variability of Antarctic sea ice is an ongoing challenge given the limitations of observed data. Coupled climate model simulations present the opportunity to examine this variability in Antarctic sea ice. Here, the daily sea ice extent simulated by the newly-released National Center for Atmospheric Research Community Earth System Model Version 2 (CESM2) for the historical period (1979–2014), is compared to the satellite-observed daily sea ice extent for the same period. The comparisons are made using a newly-developed suite of statistical metrics that estimates the variability of the sea ice extent on timescales ranging from the long-term decadal to the short term, intraday scales. Assessed are the annual cycle, trend, day-to-day change, and the volatility, a new statistic that estimates the variability at the daily scale. Results show that the trend in observed daily sea ice is dominated by sub-decadal variability with a weak positive linear trend superimposed. The CESM2 simulates comparable sub-decadal variability but with a strong negative linear trend superimposed. The CESM2's annual cycle is similar in amplitude to the observed, key differences being the timing of ice advance and retreat. The sea ice begins its advance later, reaches its maximum later and begins retreat later in the CESM2. This is confirmed by the day-to-day change. Apparent in all of the sea ice regions, this behavior suggests the influence of the semi-annual oscillation of the circumpolar trough. The volatility, which is associated with smaller scale dynamics such as storms, is smaller in the CESM2 than observed.

Plain Language Summary

Antarctic sea ice is strongly variable in space and in time. Lack of observed data makes it difficult to determine what causes this variability and limits our ability to understand the variability and to project how it might change in the future. Climate models give the opportunity to study the sea ice and to project change. We compare the sea ice simulations produced by the National Center for Atmospheric Research (NCAR) Community Earth System Model Version 2 (CESM2) with satellite-observed data for the years 1979–2014. We examine the annual cycle, trend, day-to-day change in sea ice and the volatility, a new statistic that estimates the variability at the daily scale. We show that the CESM2 is able to simulate sub-decadal variability comparable to that apparent in the observed sea ice but not the weak, positive, linear trend. The CESM2 also simulates an annual cycle of similar amplitude to that observed but the ice starts growing later and retreating later in the CESM2 than is observed. This difference in timing in the annual cycle occurs in the sea ice all around Antarctica, which suggests that it might be because of a circum-Antarctic atmospheric circulation feature called the circumpolar trough.

1 Introduction

Each year, the total Antarctic sea ice extent (SIE) grows for approximately 225 days to its maximum at the end of winter and retreats for 140 days to its minimum at the end of summer (Handcock & Raphael, 2020), describing what is arguably the most pronounced annual cycle on earth. Embedded within this regularity are regional and temporal variations (e.g., Stammerjohn et al., 2012; Raphael & Hobbs, 2014; Hobbs et al., 2016) that have significance for the Antarctic and global climate. However, aspects of its large scale variability while closely observed, are still not well understood. These include the positive trend in SIE that occurred over the satellite era until 2016 when anomalously early retreat of the sea ice led to record low SIE which continued in subsequent years (Parkinson, 2019; Meehl et al., 2019; Wang et al., 2019; Schlosser et al., 2018). There is a critical need for long term data within which to place such variability into context and to provide a basis for projecting future sea ice variability because of the important role that Antarctic sea ice plays in our closely coupled climate system. In the absence of such long term data, coupled climate model simulations present the opportunity to examine this variability in Antarctic sea ice and also to project future sea ice climate. The models have had some success in simulating the climate. For example, in their analysis of CMIP5 coupled climate models Holmes et al. (2019) have identified one model that exhibits realistic behavior. This model is able to match observations of sea ice drift. They use this to argue that the existing climate models are sophisticated enough to represent aspects of Antarctic sea ice correctly. However, while this is a significant step forward, coupled climate models have had limited success in simulating correctly fundamental aspects of the observed annual cycle and the long term trend. An assessment of the coupled climate models that were contributed to the fifth phase of the Coupled Model Intercomparison Project (CMIP5) found that many of the models had an annual SIE cycle that differed markedly from that observed over the last 30 years (Turner et al., 2013; Zunz et al., 2013). The majority of models had a SIE that was too small at the minimum in February, while several of the models exhibited much smaller SIE than observed at the September maximum. All of the models had a negative trend in SIE since the mid-twentieth century (contrary to observed) (Turner et al., 2013). For the same suite of models Roach et al. (2018) found that the sea ice concentration (SIC) from which the SIE is calculated was not well represented, for example, being too loose and low-concentration all year. They attribute this to the sea ice thermodynamics used in the models. Antarctic sea ice is intimately tied to the Antarctic climate and these biases in simulated sea ice affect the simulated climate (Bracegirdle et al., 2015). Therefore the inability of the models to simulate historical sea ice correctly limits the confidence that we might have in their projections of future climate.

In this current study we analyze the Antarctic sea ice simulated by the National Center for Atmospheric Research (NCAR) Community Earth System Model Version 2 (CESM2) (Danabasoglu et al., 2020). The CESM2 is a fully-coupled, community, global climate model that provides state-of-the-art computer simulations of the Earth's past, present, and future climate states. It is one of the coupled climate models that have been contributed to the sixth phase of the Coupled Model Intercomparison Project (CMIP6; Eyring et al., 2016). Other studies have assessed other aspects of the CESM2 Antarctic climate, including the influence of new sea ice physics (Bailey et al., 2020) and variability characteristics in the pre-industrial climate (Singh et al., 2020). Here we focus on how this model's simulation of Antarctic sea ice variability compares with observations. Our comparisons focus on the time period 1979–2014, which represents a subset of the historical runs and which coincides with the bulk of the period of satellite record. We assess the simulations using a suite of statistical metrics developed by Handcock and Raphael (2020) that allow us to to look at the variability on timescales ranging from the long-term decadal to the short term intra-day scales. We focus especially on the annual cycle and the trend, the two most significant components of variability in Antarctic sea ice, and as mentioned above, components which climate models have had difficulty reproducing. The data and method are presented in Section 2. The results are presented and discussed in Section 3 and the work is summarized and conclusions are made in Section 4.

2 Data and Method

Here we use a subset of the CESM2 historical (1850–2014) simulations, 1979–2014, from ten ensemble members and compare it with satellite-observed sea ice data from Nimbus-7 SMMR and DMSP SSM/I-SSMIS. Specifically, we used the Bootstrap Version 3 concentration fields (Comiso, 2017) from the "NOAA/NSIDC Climate Data Record of Passive Microwave Sea Ice Concentration, Version 3" (Peng et al., 2013; Meier et al., 2017) for the same period. The structural details of the CESM2 are elaborated upon in other papers in this CESM2 special collection (Danabasoglu et al., 2020) so are not discussed here.

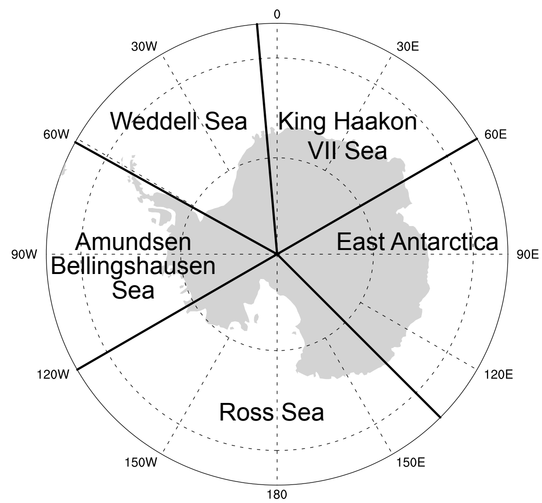

Figure 1. Sea Ice Sectors around Antarctica. Based on Raphael and Hobbs (2014).

Daily sea ice extent (SIE) for the CESM2 ensemble mean as well as for the individual ensemble members are compared with the daily SIE from the SSMI data. The SIE is calculated using the limit of the 15% SIC isoline. Thus, it is the sum of the area of every grid cell that is 15% or more covered with sea ice. The use of daily data here is new as previous model comparisons have typically used monthly averaged values. However, daily data has the potential to give much added information about the sea ice variability simulated by the model at a much finer temporal resolution. Also, much of the variability in contemporary Antarctic sea ice occurs at sub-monthly scales making the examination of daily data particularly useful. For simplicity, most of the discussion of the results focuses chiefly on the model ensemble means.

The components of variability of the SIE that are assessed are the annual cycle, trend, day-to-day change and the *volatility*. Comparisons to the long term trends may be challenging due to the role of internal variability (e.g., Polvani & Smith, 2013; Mahlstein et al., 2013). However, looking across multiple ensemble members allows some insight on whether the model can simulate a combination of external forcing and internal variability that is comparable to observations. While the annual cycle and trend are the two components most usually assessed, the day-to-day change and the volatility are new. This is largely because most analyses have been conducted on monthly or seasonal averages. The volatility is a new metric developed in Handcock and Raphael (2020). The sea ice record on any given day is the sum of a number of components of variation. These are the inter-annual variation, the annual cycle for that day, day-to-day variation and the volatility (or statistical error) in the observed daily value. Normally that magnitude of the error is considered or represented as a constant over time. However, here, we allow it to vary, explicitly representing it as a calendar time varying component. We define it as the daily standard deviation which is the intra-day variation in the sea ice extent. The volatility in the observed data is considered to be due largely to factors like the ephemeral dynamic effects of storms at the ice edge and wave-ice interactions. Some, smaller, portion of it may be due also to instrumentation and algorithm effects.

Antarctic sea ice distribution varies regionally, therefore our analysis examines the total SIE as well as the regional SIE variability in order to get a comprehensive sense of the model's performance. The sea ice regions used in this analysis (Figure 1) were defined by Raphael and Hobbs (2014) and are based on coherent spatial variability in the sea ice concentration field. DuVivier et al. (2020) assesses the seasonal distribution of sea ice concentration simulated by the CESM2. They show that the model does a credible job of simulating the distribution of sea ice concentration. Antarctic sea ice variability is closely tied to the variability in sea level pressure (SLP) over the Southern Ocean (Enomoto & Ohmura, 1990). Using SLP, taken from the ERA-Interim Reanalyses for the period 1979–2014, we make a preliminary diagnosis of reason for the differences between the simulated and observed SIE. We compare the simulated SLP with the corresponding variable in the ERA-Interim dataset.

3 Results

3.1 Trend

It is common in climate science to represent variability at sub-decadal or longer timescales as linear functions of time. In this case the presence of a non-zero slope is evidence of change. Here we expand the representation to allow non-linear functions of time, specifically, slowly changing curvilinear functions of time. This allows more flexible and realistic representations of change while retaining linear trends as a special case. Our trend is explicitly defined in equation (15) of Handcock and Raphael (2020). As we show below, this curvilinear trend captures variability at sub-decadal timescales.

Very few climate models that participated in the previous CMIPs have been able to simulate the observed positive linear trend in Antarctic SIE that occurred from 1979–2016 (e.g., Turner et al., 2013; Shu et al., 2015). One suggested reason for this discrepancy is the possibility that the processes underlying the increase in sea ice extent are not correctly represented in the models (e.g., Turner et al., 2013; Sigmond & Fyfe, 2014). Another is that the observed increase in sea ice extent might be due to natural variability rather than external forcing in the system and therefore, that the climate models do not simulate it is not necessarily a failure of the models (e.g., Polvani & Smith, 2013; Mahlstein et al., 2013). Figure 2a, which shows change in SIE associated with the trend, illustrates that as was the case for the majority of the CMIP5 models, this most recent version of CESM2 simulates a pronounced negative linear trend. This is true in the ensemble mean (thick blue line) and also apparent in each ensemble member (thin black lines). However, Figure 2b which shows the observed daily linear trend in total Antarctic SIE demonstrates that this observed positive linear trend is quite weak and may be strongly influenced by the record maxima which occurred from 2012–2014. Interestingly, Figure 2b also suggests that this level of variability of daily SIE is better represented as a curvilinear function of time rather than a linear one, suggesting variability at sub-decadal timescales. The linear trend does not provide a good characterization of the data because of these sub-decadal variations. The CESM2 simulates a comparable sub-decadal variability (Figure 2a, indeed the variability in the simulated version is much more pronounced than observed. The sub-decadal variability in the daily SIE in this current analysis is consistent with that discussed by Simpkins et al. (2013) in their analysis of changes in the magnitudes of the sea ice trends in the Ross and Bellingshausen Seas. That the CESM2 is successful at simulating sub-decadal variability in the SIE suggests that the model may be used for diagnosing the mechanisms that force this nonlinear behavior.

We also examine the simulated and observed trends by region. Shown in Figure 3 are the observed and ensemble mean simulated trends. The curvilinearity apparent in the observed total SIE (Figure 3a) is also noted regionally as is expected. It is most pronounced in the Weddell and Ross sectors, which also show the largest changes, followed by King Haakon VII Sea, East Antarctica and the Amundsen-Bellingshausen (ABS) sectors. It is interesting to note that the timing of the sub-decadal variation is not synchronous in some regions, a fact best illustrated by the Ross and Weddell Sea sectors (Figure 3a). This dipole of variability between the Weddell and Ross sectors is reminiscent of the Antarctic Dipole, the leading mode of interannual variability in Antarctic sea ice (e.g., Yuan & Martinson, 2000, 2001; Holland et al., 2005). Given that these two sectors contribute most to the total SIE, such lack of synchronicity has a potentially damping effect on the trend in total SIE. Regionally, the CESM2 captures the range of the trends in terms of

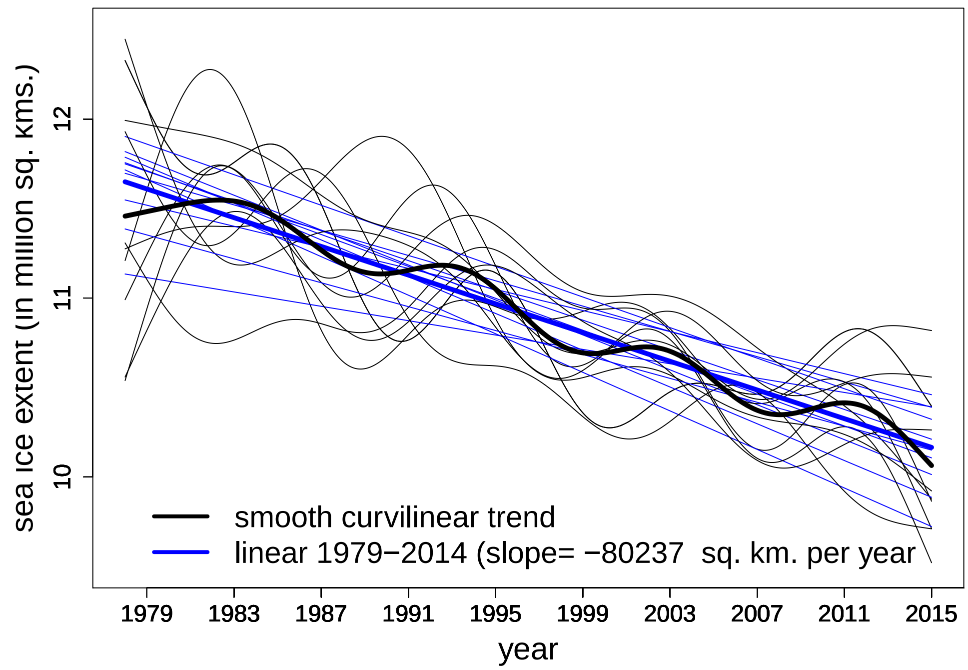

(a)

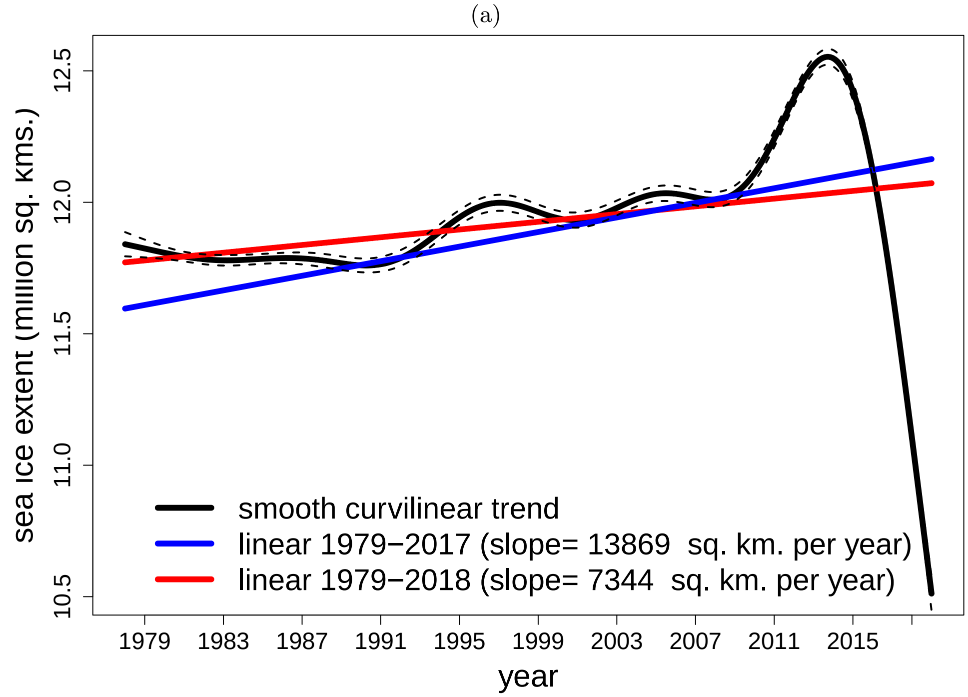

(b)

Figure 2. Observed and simulated trends in daily Antarctic sea ice extent represented in terms of the area of sea ice involved in the trend. a) Curvilinear (black) and linear (blue) trends simulated by the CESM2. Bold lines are the ensemble mean, thin lines are the individual ensemble members; b) Observed trends in daily Antarctic sea ice–linear trend from 1979–2017 (blue), from 1979–2018 (red); curvilinear trend (black) with 95% pointwise confidence intervals (dashed black lines).

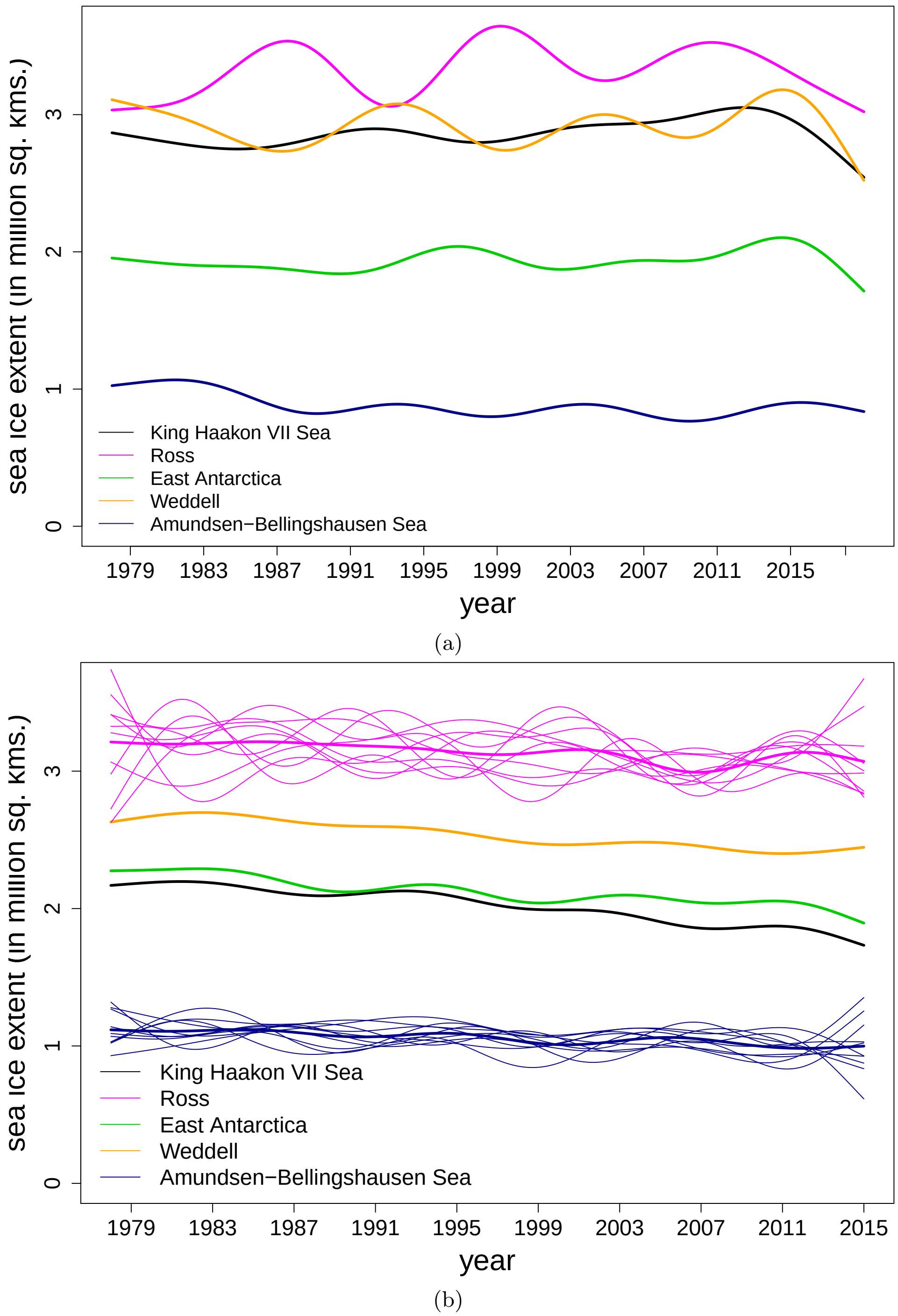

Figure 3. Regional observed and simulated trends in daily Antarctic sea ice extent. a) Observed trends; b) Trends simulated by the CESM2. Regions are Amundsen-Bellingshausen sector (dark blue), East Antarctica (green), Weddell Sea (orange), King Haakon VII Sea (black); Ross Sea (magenta). The thin blue and magenta lines are the individual ensemble members for the Ross and Amundsen-Bellingshausen sectors, respectively. On the horizontal axis is time. On the vertical axis is the change in sea ice extent due to the trend.

the area of sea ice involved. As is observed, the simulated ABS sector has the smallest effect while the Ross sector has the largest in terms of the area of sea ice. The simulated trend in the King Haakon VII Sea sector is weaker than observed and now comparable to the neighboring East Antarctica sector. Both Singh et al. (2020) and DuVivier et al. (2020), show that the SIE simulated by the CESM2 in the King Haakon VII Sea sector is smaller than observed, particularly in winter. This can be expected to reduce the area of sea ice involved in the trend for this sector. The curvilinearity in the ensemble mean time-series of the CESM2's SIE is apparent at the regional scale (Figure 3b) but much weaker in general than observed, especially in the ABS. A good proportion of this is due to averaging of the curvilinearity of the ensemble members. To illustrate this we show the ensemble members for the Ross (thin, magenta lines) and the ABS (thin, dark blue lines). It seems clear, especially for the Ross that individual ensemble members are more variable than the mean. However, calculations of the average variance of the curvilinearity of ensemble members show that the Ross, Weddell and Amundsen-Bellingshausen Sea sectors have lower variance than the observed, while the King Haakon VII Sea and East Antarctica exhibit more (The variance ratios are 0.66, 0.37, 0.88, 1.28, 1.25, respectively).

3.2 Annual cycle

Here we compare the amplitude (the difference between the maximum and minimum extents), and phase (the timing of the advance and retreat) of the observed, daily annual cycle of SIE with that simulated by CESM2. The amplitude and phase are the two key characteristics of the annual cycle of sea ice. The traditional way of calculating the annual cycle is to take the average SIE for each day of the year. However, an annual cycle produced in this fashion does not include the effect of the day preceding nor the day following the averaged day, therefore it disguises the fact that the phase may be changing slowly and that the amplitude as well as the shape of the annual cycle might vary. Given these limitations we consider an annual cycle that allows variation for amplitude and phase. It assumes that the phase, which is the timing of advance and retreat of the ice, varies continuously while the amplitude varies annually. In this way, the annual cycle is not constrained to be a fixed (in time) cyclical pattern. Instead, the amplitude and shape of the cycle are allowed to vary, as would occur naturally. Specifically, the annual cycle is modeled as a cyclic cubic spline function of the phase of the cycle with an amplitude that varies annually. The phase is modeled as a slowly changing smooth function of the day-of-the-cycle, with the smoothness estimated from the data. The mathematical details of the annual cycle and its estimation are given in Handcock and Raphael (2020), Section 3.1. The outcome, averaged over the dataset period, is shown in Figure 4a and presents a more thorough if nuanced description of the annual cycle than the traditional daily climatology. For clarity, Figure 4 shows only the ensemble mean and the observed cycles. On the horizontal axis is the day of the cycle, not the day of year. Day 1, which is the average day on which the sea ice stops retreating and begins to advance is Julian day 50. Figure 4a shows that the simulated SIE is much smaller than the observed during the period of ice advance, and especially at sea ice minimum and maximum. This result is similar to what was found in some models in the CMIP5 suite (e.g., Turner et al., 2013) and more recently in some of the CMIP6 suite of models (Roach et al., 2020). Moreover, it shows clearly that the sea ice minimum in the CESM2 occurs after ice has begun its advance in the observed cycle and that there are small differences during the retreat phase of the ice. Given that the annual cycle in the model is starting later and from a lower minimum it is possible that the model is simulating an amplitude, i.e a difference between the SIE at maximum and minimum, that is within range of that observed.

To examine more closely the apparent differences in amplitude and phase shown on Figure 4a, we consider a variant of the annual cycle that allows for variation in amplitude while having invariant phase. This is the amplitude adjusted annual cycle, de-

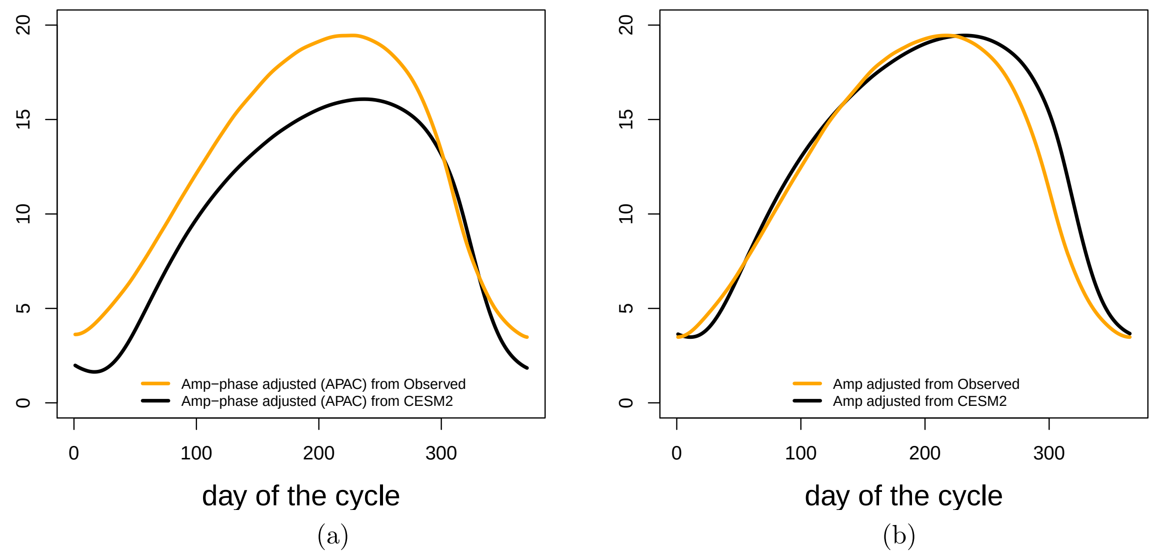

Figure 4. Observed and simulated annual cycles. a) Amplitude and phase adjusted annual cycles (APAC); b) Amplitude adjusted annual cycles. CESM2 (black lines), Observed (orange lines). On the horizontal axis is day of cycle – day 0 is Julian Day 50. On the vertical axis is sea ice extent in millions of square kilometers. See Handcock and Raphael (2020) for more information on the annual cycles.

tailed in Handcock and Raphael (2020), Section 3.1. This is similar to the amplitude-phase adjusted annual cycle (APAC), but allows the phase differences to be identified. Figure 4b shows that the amplitude is of comparable size as suggested earlier. The obvious difference is that of the phase in the retreat period. We note that this difference in phase is hinted at in Figure 4a but is not as obvious perhaps because the apparent amplitude difference is dominant. This phase difference also appears (but is not discussed) in the monthly analysis carried out by DuVivier et al. (2020). They show that sea ice retreat in the CESM2 begins in October rather than September. In the advance period (Figure 4b), the sea ice in CESM2 begins advancing some days later than the observed but catches up quickly and the rate of advance appears to be more or less the same for most of the growth phase of the ice. There is however, a clear difference in phase for the latter part of the ice cycle. During this time, the observed sea ice begins to retreat at day of cycle 215 (Julian Day 266), 12 days earlier than the CESM2 ensemble mean simulations. To put this in recent context, the anomalously early retreat of sea ice in 2016 began approximately three weeks before the median retreat onset. This points to the benefit of using daily data, as these differences would not be adequately resolved using monthly means.

The amplitude adjusted annual cycles are also examined for each region alongside the total SIE for comparison (Figure 5). The regional cycles, both simulated and observed, exhibit marked differences in the shape and length of the annual cycles which demonstrate why it is important to study Antarctic sea ice variability from a regional perspective. These annual cycles differ in the timing of the start and rate of advance, the time spent at maximum and the start and rate of retreat. Some of these differences are quantified in Table 1 which gives the day that SIE maximum is achieved for the observed and CESM2 for each sector in Julian days. In the observed, the timing of maximum SIE is quite varied. First to achieve maximum is the ABS, followed closely by the Weddell. The King Haakon VII Sea sector achieves maximum SIE last, more than a month after the ABS sector. The shape of the annual cycle of the ABS is unusually peaked compared to the others because the ice grows rapidly to maximum, and spends very little time there

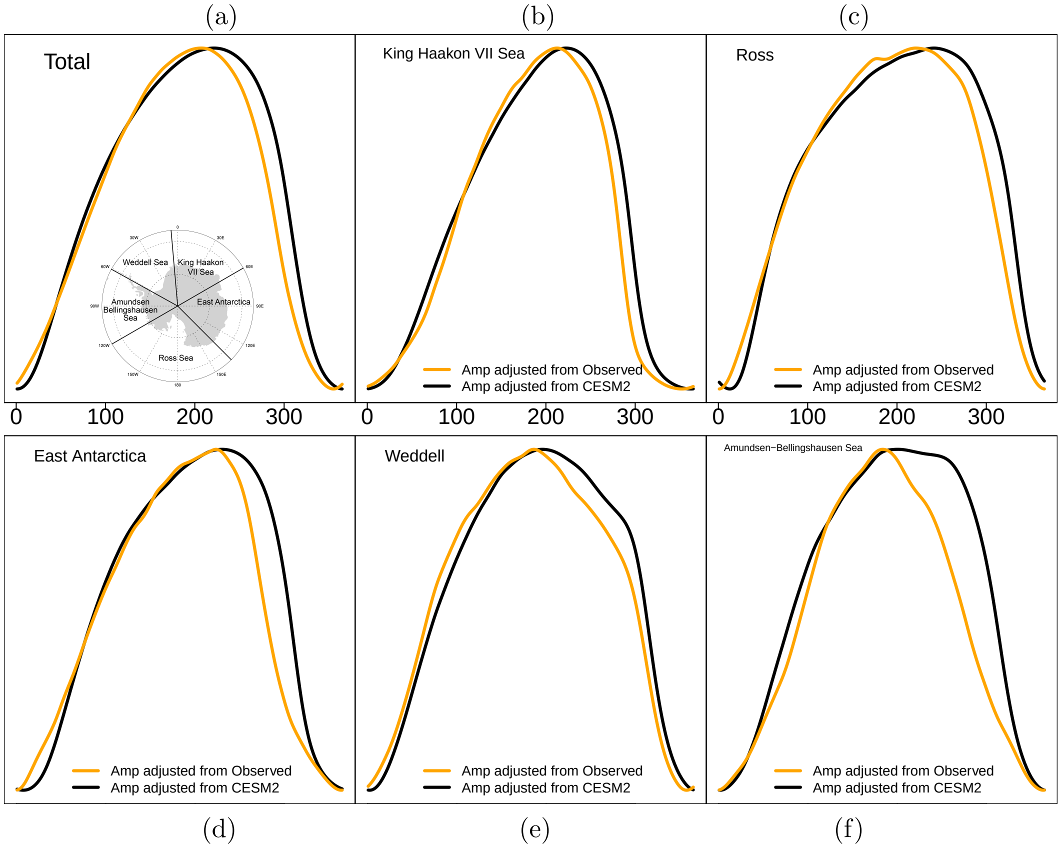

Figure 5. Total and Regional observed and simulated amplitude-adjusted annual cycles. a) Total sea ice extent. b) King Haakon VII Sea, c) Ross Sea, d) East Antarctica, e) Weddell Sea, f) Amundsen-Bellingshausen Sea. On the horizontal axis is day of cycle – day 0 is Julian Day 50. On the vertical axis is the annual cycle of the sea ice extent. Each vertical axis has the same standardized scale of 0 to 1.

before retreat begins. This is also true but is not as pronounced for the Weddell and King Haakon VII Sea sectors. In the CESM2 the timing of retreat varies across the regions similarly to the observed, except that SIE in King Haakon VII Sea sector begins its retreat earlier than the SIE in the Ross. Here we define the onset of retreat as the day after the SIE reaches its maximum. One measure of the delay in timing of the retreat is the difference in the onset of retreat for the observed SIE and CESM2 SIE. The last column of Table 1 shows this delay in retreat which is also visible in Figure 5 (It is easier to see in the day-to-day changes in Figure 6, the subject of the next section). This delay is longest in the Ross which begins to retreat approximately one month after the observed, and shortest in East Antarctica which experiences a delay of only six days.

These regional differences in the shape and length of the annual cycle are interesting to explore, and indicate that there is much to learn about Antarctic sea ice variability at the regional scale. Certainly the fact that each sea region is influenced by different components of the large scale atmospheric circulation (Raphael & Hobbs, 2014) during ice advance and retreat can provide some explanation here. It is also quite likely that the state of the ocean exerts some influence. The comparison of the annual cycles of the observed and the CESM2 yields one striking similarity; they all have in common the phase difference seen in the total SIE. That is, sea ice begins to retreat later in the model than observed in each of the regions. Even here there are interesting differences, notably in the Weddell and the ABS regions. In both these regions the start of retreat is later and

Table 1. Days-of-the-year for Annual Cycle Events[a]

	Observed			CESM2			
	Advance	Maximum	Retreat	Advance	Maximum	Retreat	Delay
Total	125	266	352	103	282	3	16
King Haakon VII Sea	166	280	349	124	295	362	15
Ross	87	267	5	97	297	18	30
East Antarctica	125	277	323	102	283	364	6
Weddell	121	244	4	102	259	9	15
ABS	168	241	343	118	254	11	13

[a]Regional observed and simulated Julian day-of-the-year for the date of maximum SIE advance rate, maximum SIE and maximum SIE retreat rate. The last column is the number of days delay in the start of SIE retreat from observed to simulated.

slower than observed. The slower rate of retreat is likely linked to thicker ice that develops in the ABS and Weddell sectors in winter and lingers into summer(Singh et al., 2020). Thicker ice also develops in the Ross sector in winter but it does not last into summer which is probably why the annual cycle for the Ross is closer in shape to the observed.

That the difference in phase is consistent in all of the regions around the continent suggests that it is due to a large-scale rather than regional mechanism. A potential agent is the semi-annual oscillation (SAO) of the circumpolar trough (CPT). Earlier studies suggest that the SAO modulates the advance and retreat of the ice because it influences the location of the westerly and easterly surface winds which in turn promote or limit the spread of the ice (e.g., Enomoto & Ohmura, 1990; Stammerjohn et al., 2003). This is explored below.

3.3 Day-to-day change in SIE

The simulated day-to-day change in SIE has not been compared with observed data before. It is essentially the derivative of the annual cycle. It gives insight into the rate of daily advance and retreat of the ice and in doing so becomes an expression of the phase. Shown in Figure 6, positive values of the day-to-day change indicate that ice is advancing while negative values indicate that ice is retreating. Zero advance (retreat) occurs at maximum (minimum). Growth in the observed total SIE (Figure 6a) begins quickly before slowing to maximum near Julian day 266. The retreat is faster than the advance. This describes a well-known characteristic of the Antarctic sea ice cycle — a relatively slow growth to maximum followed by a rapid retreat. This daily analysis, seen in all of the regions as well as the total SIE, shows that the rate of ice advance is not monotonic, but the rate of retreat is monotonic both when it is increasing and decreasing.

As might be expected from the analysis above, there are clear regional differences in the observed day-to-day change in SIE (Figure 6b–f). The King Haakon VII Sea sector (Figure 6b) sustains the most rapid rates of advance and retreat while the ABS sector shows the least. This latter behavior in the ABS sector might be related to the fact that this sector has the smallest SIE. Table 1 gives the Julian days of maximum advance and maximum retreat and of maximum SIE by region.

As shown by the ensemble mean (Figure 6a), the simulations capture the general shape of the day-to-day changes in ice but there are important differences. SIE in the CESM2 starts advancing later, from a lower value, but achieves its peak growth rate earlier (see Table 1), and has a maximum growth rate that is higher than the observed. Once its peak growth rate is achieved however, it continues to grow more slowly than the observed for the rest of its advance. It begins retreat later, achieving a maximum rate of retreat that is faster and later in the cycle than is observed (see Table 1), continuing to retreat after the observed has begun to advance. The day-to-day change in Figure 6a is

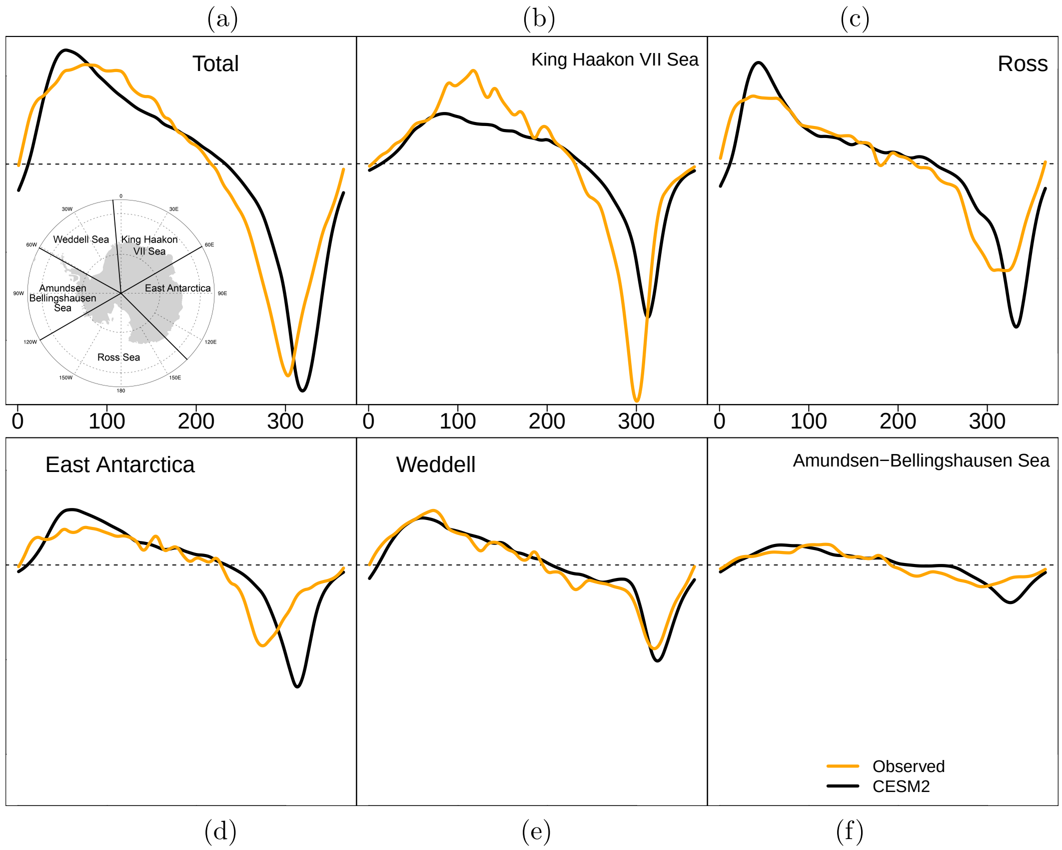

Figure 6. Total and Regional observed (orange) and simulated (black) day-to-day change in Antarctic sea ice. a) Total sea ice extent. b) King Haakon VII Sea, c) Ross Sea, d) East Antarctica, e) Weddell Sea, f) Amundsen-Bellingshausen Sea. On the horizontal axis is day of cycle – day 0 is Julian Day 50. On the vertical axis is rate of change of the sea ice extent in millions of square kilometers per day. The vertical axes on panels (b)-(f) are the the same.

consistent with the annual cycle shown in Figure 4, especially with the phase differences seen in Figure 4b. Additionally, it suggests that the very low minimum SIE achieved by the CESM2 is related to the high, late stage, maximum decay rate.

Regionally, the day-to-day changes (Figure 6b–f) display grossly similar characteristics to the total SIE. The sea ice retreat begins later in CESM2 in each region (typically 2 weeks; See the last column of Table 1). The maximum rate of retreat also occurs later in CESM2 (typically 2 weeks; Table 1); this is most pronounced in the East Antarctica sector (41 days), least in the Weddell Sea (5 days). The Weddell Sea sector is most similar to the observed, achieving its maximum extent and maximum rate of retreat at approximately the same days, while the King Haakon VII Sea sector is the most different. Unlike the other sectors, its advance and retreat rates are lower than observed. This might be related to the smaller SIE simulated by the CESM2 in the King Haakon VII Sea sector (DuVivier et al., 2020; Singh et al., 2020). In the ABS, the extended lag noted in Figure 5f shows up as an extended period of little change at maximum in the CESM2 while during that same period the observed SIE was retreating. The East Antarctica and Ross sectors are quite similar to the observed but have later and greater maximum rate of decrease. Overall the regional day-to-day changes are consistent with shape and the regional phase differences seen in the amplitude-only adjusted annual cycles in Figure 5.

3.4 Volatility

The sea ice volatility, the daily standard deviation in the sea ice simulated by the coupled climate models, has not been evaluated before. However, as shown in Figure 7, it can be responsible for fluctuations at the ice edge on the order of 40,000 – 50,000 km^2 which, while small compared to the total SIE, becomes significant at the regional scale and when compared to the size of the sea ice grid box. The volatility is considered to be due mainly to the dynamic effects of storms, ocean circulation (eddies) and wave-ice interaction at the ice edge. Stammerjohn et al. (2003) suggest that dynamics rather than thermodynamics initiate and dominate anomalies along the ice edge. The total observed volatility (Figure 7a) is lowest during the early stages of ice advance, large at SIE maximum and achieves a second, larger maximum later in the cycle, during the days of fastest sea ice retreat. The increased volatility at SIE maximum may be associated with the peak in storm activity in the southern winter discussed by Carleton (1979) and Simmonds and Keay (2000). These storms cause fluctuations at the sea ice edge rather than within the pack where the sea ice concentration is at or close to 100%. Therefore, the apparent cycle in volatility may be due to the effect of storms at the ice edge. The second peak which occurs shortly after the maximum rate of retreat (indicated by the green line) might also be dynamically induced, which would be consistent with the finding of Kusahara et al. (2018) that the retreat of Antarctic sea ice (except in the Ross Sea) is largely wind driven.

Regionally, the observed double peak is strongly apparent in the King Haakon VII Sea sector, and more weakly in the Weddell and Ross sectors. It is interesting that East Antarctica and the ABS sectors have only one, pronounced peak at the SIE maximum before shrinking quite rapidly to a minimum near the end of the cycle. This lack of a second peak in volatility in the ABS might simply be due to the lack of sea ice in those regions at that stage of the cycle.

Overall, the volatility of total SIE in the CESM2 is lower than the observed by approximately 20,000 km^2 per day and the cycle of volatility is also weak. The simulated volatility increases early during ice advance, but instead of climbing to a maximum, it maintains a steady state for most of the year until, like the observed, it experiences a large maximum late in the ice cycle. Regionally (Figure 7), volatility is usually lower in CESM2 except late in the retreat period in the ABS and East Antarctica. The late cycle increase in volatility occurs in all of the regions, except the ABS, and immediately follows the time of maximum decay.

The lower volatility exhibited by the CESM2 during most of the growth stage of the ice, suggests that daily dynamic forcing of ice fluctuation at the ice edge in the CESM2 is smaller than observed. This can happen if the processes that drive high frequency variability inherent in features such as storms and ocean eddies, are deficient in the model, which is a likely consequence of the relatively coarse model resolution (of about 1 degree in latitude and longitude).

3.5 The Potential role of the Semi-annual Oscillation

Integrating the information given by the comparison of the annual cycles, the day-to-day mean and the volatility we see that the CESM2 simulates an annual cycle with amplitude similar to that observed but with a retreat phase that begins later in the cycle. We also see that the simulated maximum decay rate is greater, occurs later in the cycle, and is associated with the late peak in volatility. We address now a factor that moderates the timing or phase of the annual cycle, the semi-annual oscillation (SAO). Although it has not been fully quantified, a number of studies suggest that the timing of advance and retreat of Antarctic sea ice is moderated by the SAO (Enomoto & Ohmura, 1990; Simmonds, 2003; Stammerjohn et al., 2003; Simmonds et al., 2005). An important characteristic of the southern hemisphere atmospheric circulation, the SAO is associated with more than 50% of the variability in SLP (van Loon & Rogers, 1984; Taschetto et

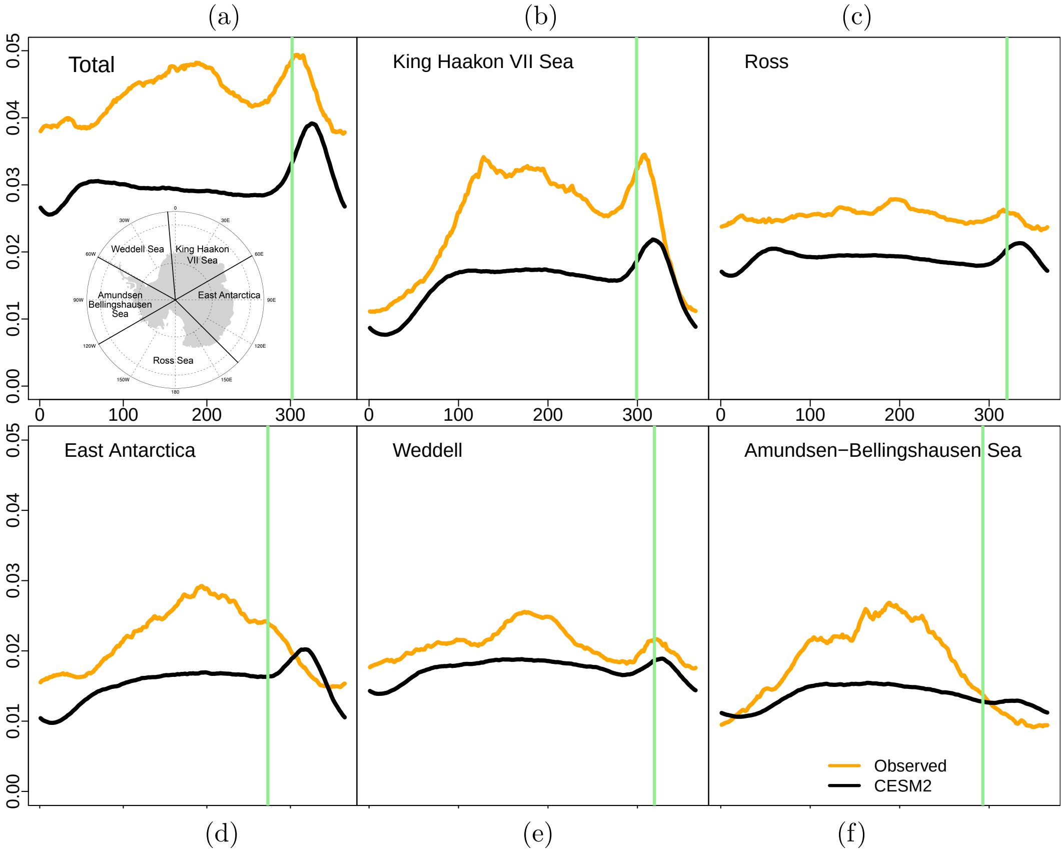

Figure 7. Total and Regional observed (orange) and simulated (black) volatility in Antarctic sea ice. a) Total sea ice extent. b) King Haakon VII Sea, c) Ross Sea, d) East Antarctica, e) Weddell Sea, f) Amundsen-Bellingshausen Sea. On the horizontal axis is day of cycle – day 0 is Julian Day 50. On the vertical axis is the daily standard deviation of sea ice extent. Each vertical axis has the scale 0 to 0.05 millions of square kilometers. The green vertical lines mark the day of maximal observed SIE retreat for that region or total (See Figure 6). The observed values are based on DMSP era data only.

al., 2007). It is expressed by the bi-annual changes in location and intensity of the circumpolar trough (CPT). As described in van Loon (1967), the CPT contracts, deepens and moves south in March and September and expands, weakens and moves north in June and December. Similar accompanying fluctuations of the tropospheric temperature gradients, geopotential heights, SLP and winds at middle and high latitudes in the SH occur. The changing wind directions associated with the meridional shift in the CPT in spring is thought to create divergence in the ice pack causing a reduction in sea ice concentration and priming the pack for rapid break up by wind and ocean late in the annual cycle (December) (Enomoto & Ohmura, 1990). Stammerjohn et al. (2003) show that the timing of the north/south migration of the CPT influences the timing of sea-ice advance and retreat via wind-driven sea-ice drift. A lucid discussion of the SAO and its influence on Antarctic sea ice can be found in Eayrs et al. (2019).

An in-depth evaluation of SAO simulated by the CESM2 within the context of sea ice variability is beyond the scope of this paper. However, given the hypothesized link between the SAO and the timing of sea ice advance and retreat, and its potential for explanation, we examined how well the CESM2 simulates the SAO, using the zonal mean SLP difference between latitudes 50S and 65S. It is a measure of the strength of the winds between those latitudes such that a large, positive value indicates stronger westerlies,

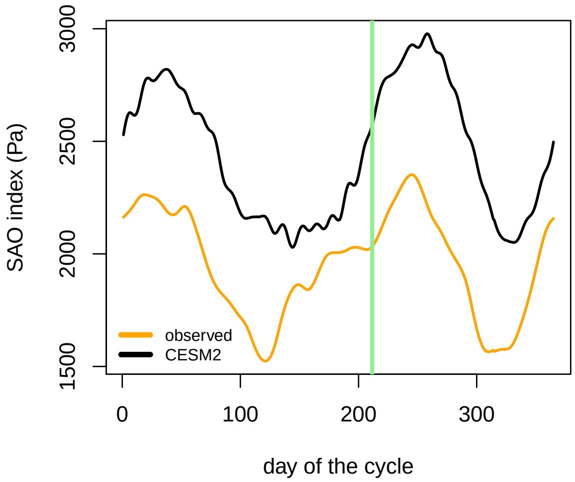

Figure 8. Semi-annual Oscillation Index: Observed (orange) and simulated (black) zonal mean SLP difference between latitudes 50S and 65S. The green line marks the observed day of onset of sea ice retreat. On the horizontal axis is day of cycle – day 0 is Julian Day 50. On the vertical axis is the zonal mean sea level pressure difference in Pa.

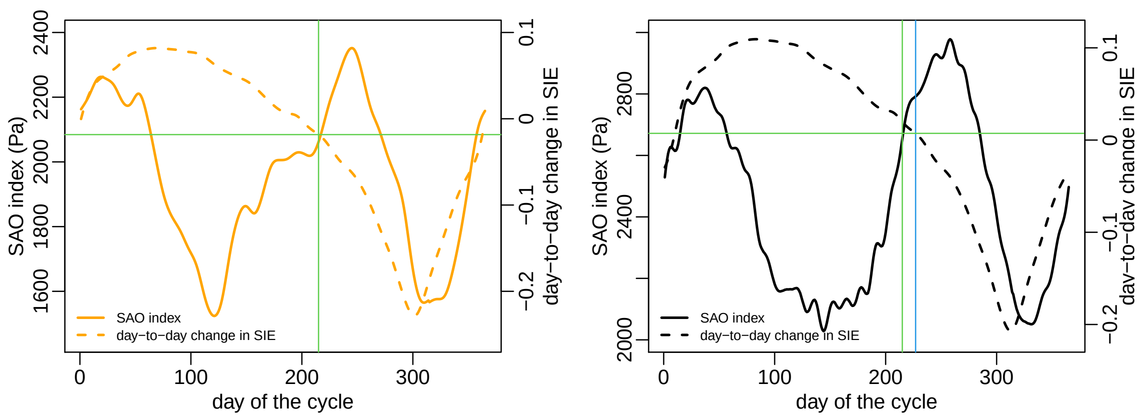

(a) (b)

Figure 9. Observed (a) and simulated (b) day-to-day change and corresponding SAO index. The green line marks the observed day of onset of sea ice retreat. The blue line marks the simulated day of onset of sea ice retreat. On the horizontal axis is day of cycle: day 0 is Julian Day 50. On the left vertical axes are the zonal mean sea level pressure differences in Pa. On the right vertical axes are the rates of change of the sea ice extent in millions of square kilometers per day

and the intensity of the CPT (Hurrell & van Loon, 1994; Meehl et al., 1998; Taschetto et al., 2007). The CESM2 (Figure 8: black line) simulates a well-defined SAO index which is different from the observed in two ways; it is always larger, indicating stronger winds and a deeper CPT, and it is offset in time so that the minimum and maximum meridional pressure gradients are achieved later in the year than observed. This means that the simulated CPT begins shifting southwards later, reaching its southernmost location and greatest intensity later than the observed CPT. The significance of this temporal offset to the timing of ice retreat becomes clearer in Figure 9a and b where the day-to-day changes in SIE are overlaid on the observed and simulated SAO indices along with the times of onset of retreat. The later retreat of ice in the CESM2 is tied to the slower southward movement of the CPT.

4 Summary and Conclusions

This study is an evaluation of the satellite-era variability in Antarctic sea ice extent simulated by the CESM2, using some newly developed metrics from Handcock and Raphael (2020). These metrics examine the variability from the long term trends to the intra-day, giving a detailed picture of the temporal variability of Antarctic sea ice extent simulated by the model. This complements work that has assessed other aspects of the Antarctic climate in pre-industrial control conditions (Singh et al., 2020). Here, we are able to explicitly diagnose differences between the model and observed, which may be used to give a sense of what elements of the model need more development. Over the historical period the trend in observed daily sea ice is dominated by a curvilinear interannual component with a weak positive linear trend superimposed. As was the case for the majority of the CMIP5 models, CESM2 simulates a strong negative trend in SIE and therefore is still in contrast to the observations, a difference which might be due to natural variability rather than a model deficiency. Analysis of the observed daily sea ice shows that the linear trend is weak and that the longer term variability in Antarctic sea ice is dominated by sub-decadal variability. The CESM2 simulates a comparable sub-decadal variability in the total SIE and well as in the individual sea ice sectors, although this is better seen in the individual ensemble members than in the ensemble mean. That the CESM2 is able to simulate comparable sub-decadal variability suggests that the model may be used to diagnose and or evaluate the factors contributing to this variability.

With respect to the annual cycle, the total SIE at time of maximum simulated by the CESM2 is lower than recorded. Since sea ice in the model begins advancing later and from a much smaller minimum than observed it might never reach the size of the observed SIE at the time of maximum. However, if the amplitude is calculated as the difference between the minimum and maximum SIE, the CESM2 does produce an annual cycle with similar amplitude to that observed. This apparent difference in amplitude between the the observed annual cycle and that of the CESM2 is the result of the complex relationship between amplitude and phase, the two key characteristics of the annual cycle. Separation of the variation of the amplitude and phase by using an amplitude-adjusted only annual cycle showed that the main difference between the simulated and observed annual cycles is the timing of ice retreat. The CESM2 reaches its SIE maximum later and begins its retreat later than observed and this is apparent in both the total and the regional SIE.

This difference in the annual cycles is echoed in the day-to-day change, a variable that has not been examined before since most analyses focus on the monthly and seasonal SIE. Here, the day-to-day change is consistent with and might be considered a proxy for the large scale elements of the annual cycle (advance/retreat), while adding precision with respect to the exact timing of advance and retreat. While the rates of change are generally similar (except for the peak rate of retreat in the CESM2 which is much larger), sea ice begins its advance and retreat later in the CESM2. An additional phenomenon not seen when looking at monthly averages, but perhaps known anecdotally, is that the rate of sea ice advance is not monotonic but the rate of sea ice retreat is monotonic when it is increasing and when it is decreasing (Figure 6). This knowledge is potentially useful when considering thermodynamic vs dynamic effects on sea ice advance and retreat.

A potential contributor to the retreat phase difference between the observed annual cycle and that of the CESM2 is the simulated semi-annual oscillation (SAO). An initial evaluation of the SAO index shows that the meridional gradient of pressure simulated by the CESM2 is larger and the maximum (and minimum) of this gradient occur later in the cycle than observed. We suggest that this is due to a deeper, slower moving Circumpolar Trough. Indeed, our analysis links the later retreat of ice in the CESM2 to the slower southward movement of the Circumpolar Trough. The influence of the SAO on sea ice variability has long been a subject of study (e.g., van Den Broeke, 2000). The differences between the CESM2 and the observed data discussed here, present an opportunity to examine closely this important atmospheric mechanism and its role in the Antarctic sea ice climate.

A novel aspect of variability compared here is the daily standard deviation, named here, the volatility (Handcock & Raphael, 2020). This measure of variability is associated with smaller scale dynamics, and is responsible for significant fluctuations in SIE at the grid scale. In the observed, it achieves a first maximum near the time of sea ice maximum and a second near the time of maximum rate of retreat of the ice. In general, this component of variability is lower in the CESM2 than observed. Also missing is the slow but clear growth in volatility to a maximum near the time of the sea ice maximum. However, the CESM2 does simulate the peak volatility associated with the very rapid rate of decay late in the ice cycle. As mid-winter sea ice variability is associated with the smaller scale dynamics such as storms (e.g., Stammerjohn et al., 2003), ocean eddies and wave-ice interaction at the ice edge, it may be that the model is not simulating these processes well, something that is common across the CMIP models. We note also that the observed sea ice grid size at 25km x 25km is much smaller than that of the CESM2's (1 degree) thus might be expected to exhibit more daily volatility than the CESM which is a 1 degree model.

Finally, the focus of this analysis has been to determine the ability of the CESM2 to simulate the key components of the variability of Antarctic sea ice and to suggest what might be the proximate cause of the differences that are seen. However, what has become even clearer in the process is that in-depth analysis of Antarctic sea ice variability requires a regional (or by sea ice sector) approach. Important differences in variability that are apparent by sector are muted or damped, when only the total SIE is considered. The sea ice sectors differ not only in the amplitude of their sea ice extents but also in their phase (or timing) of sea ice advance and retreat, and the rates of advance and retreat of the sea ice. All of these combine to present a fairly complex picture of variability. This is true of the observed as well as the simulated SIE. Raphael and Hobbs (2014) show that sea ice in each sector is influenced by different components of the large scale atmospheric circulation, both remote from, and local to, the Antarctic. The state of the ocean and the effect of the interaction between the ocean and the atmosphere on the ice must also be considered in attempts to determine the sources of these differences in Antarctic sea ice variability.

Acknowledgments

This work was supported by the National Science Foundation (NSF) under the Office of Polar Programs under grant NSF-OPP-1745089. The CESM project is supported primarily by the NSF. This material is based upon work supported by the National Center for Atmospheric Research, which is a major facility sponsored by the NSF under Cooperative Agreement No. 1852977. Computing and data storage resources, including the Cheyenne supercomputer (doi:10.5065/D6RX99HX), were provided by the Computational and Information Systems Laboratory (CISL) at NCAR. We thank all the scientists, software engineers, and administrators who contributed to the development of CESM2. LL was funded by NSF grant 1643484.

The CESM2 model output used in this study is available at the NCAR Digital Asset Services Hub (DASH; https://data.ucar.edu). The Bootstrap Sea Ice Concentration data are available at the National Snow and Ice Data Center (NSIDC) (Peng et al., 2013; Meier et al., 2017). The ERAI reanalysis data (Dee et al., 2011) are available from the Centre for Medium-Range Weather Forecasts (ECMWF).

References

Bailey, D. A., Holland, M. M., DuVivier, A. K., Hunke, E. C., & Turner, A. K. (2020). *Impact of a new sea ice thermodynamic formulation in the CESM2 sea ice component.* (Manuscript submitted for publication to the *Journal of Advances in Modeling Earth Systems*)

Bracegirdle, T. J., Stephenson, D. B., Turner, J., & Phillips, T. (2015). The importance of sea ice area biases in 21st century multimodel projections of antarctic temperature and precipitation, geophys. *Geophysics Research Letters*, *42*(10), 832-839. doi: 10.1002/2015GL067055

Carleton, A. M. A. (1979). Synoptic climatology of satellite-observed extratropical cyclone activity for the southern hemisphere winter. *Archives for meteorology, geophysics, and bioclimatology*, *27*, 265-279.

Comiso, J. (2017). *Bootstrap sea ice concentrations from NIMBUS-7 SMMR and DMSP SSM/I-SSMIS, Version 3.* NASA National Snow and Ice Data Center Distributed Active Archive Center. doi: 10.5067/7Q8HCCWS4I0R

Danabasoglu, G., Lamarque, J.-F., Bacmeister, J., Bailey, D. A., DuVivier, A. K., Edwards, J., ... Strand, W. G. (2020). The community earth system model Version 2 (CESM2). *Journal of Advances in Modeling Earth Systems*, *12*(2), e2019MS001916. doi: 10.1029/2019MS001916

Dee, D. P., Uppala, S. M., Simmons, A. J., Berrisford, P., Poli, P., Kobayashi, S., ... Vitart, F. (2011). The era-interim reanalysis: configuration and performance of the data assimilation system. *Quarterly Journal of the Royal Meteorological Society*, *137*(656), 553-597. doi: 10.1002/qj.828

DuVivier, A. K., Holland, M. M., Kay, J. E., Tilmes, S., Gettelman, A., & Bailey, D. A. (2020). *Arctic and antarctic sea ice state in the community earth system model version 2.* Manuscript submitted to JGR-Oceans.

Eayrs, C., Holland, D. M., Francis, D., Wagner, T. J. W., Kumar, R., & Li, X. (2019). Understanding the seasonal cycle of antarctic sea ice extent in the context of longer-term variability. *Reviews of Geophysics*, *57*, 1037-1064.

Enomoto, H., & Ohmura, A. (1990). The influences of atmospheric half-yearly cycle on the sea ice extent in the antarctic. *Journal of Geophysical Research: Oceans*, *95*(C6), 9497-9511. doi: 10.1029/JC095iC06p09497

Eyring, V., Bony, S., Meehl, G. A., Senior, C. A., Stevens, B., Stouffer, R. J., & Taylor, K. E. (2016). Overview of the coupled model intercomparison project phase 6 (cmip6) experimental design and organization. *Geoscientific Model Development*, *9*(5), 1937–1958. doi: 10.5194/gmd-9-1937-2016

Handcock, M. S., & Raphael, M. N. (2020). Modeling the annual cycle of daily antarctic sea ice extent. *The Cryosphere*, *14*(7), 2159–2172. doi: 10.5194/tc-14-2159-2020

Hobbs, W. R., Massom, R., Stammerjohn, S., Reid, P., Williams, G., & Meier, W. (2016, August). A review of recent changes in Southern Ocean sea ice, their drivers and forcings. *Global and Planetary Change*, *143*, 228-250. doi: 10.1016/j.gloplacha.2016.06.008

Holland, M. M., Bitz, C. M., & Hunke, E. C. (2005). Mechanisms forcing an antarctic dipole in simulated sea ice and surface ocean conditions. *Journal of Climate*, *18*(12), 2052-2066. doi: 10.1175/JCLI3396.1

Holmes, C. R., Holland, P. R., & Bracegirdle, T. J. (2019). Compensating biases and a noteworthy success in the CMIP5 representation of antarctic sea ice processes. *Geophysical Research Letters*, *46*, 4299-4307.

Hurrell, J. W., & van Loon, H. (1994). A modulation of the atmospheric annual cycle in the southern hemisphere. *Tellus*, *46A*, 325-338.

Kusahara, K., Williams, G., Massom, R., Reid, P., & Hasumi, H. (2018, 07). Spatiotemporal dependence of antarctic sea ice variability to dynamic and thermodynamic forcing: A coupled ocean–sea ice model study. *Climate Dynamics*. doi: 10.1007/s00382-018-4348-3

Mahlstein, I., Gent, P. R., & Solomon, S. (2013). Historical antarctic mean sea ice area, sea ice trends, and winds in CMIP5 simulations. *Journal of Geophysical Research: Atmospheres*, *118*(11), 5105-5110. doi: 10.1002/jgrd.50443

Meehl, G. A., Arblaster, J. M., Chung, C. T. Y., Holland, M. M., DuVivier, A., Thompson, L., ... Bitz, C. M. (2019). Sustained ocean changes contributed to sudden antarctic sea ice retreat in late 2016. *Nature Communications*, *10*(1), 14. doi: 10.1038/s41467-018-07865-9

Meehl, G. A., Hurrell, J. W., & H. van Loon, A. (1998). Modulation of the mechanism of the semiannual oscillation in the southern hemisphere. *Tellus*, *50A*, 442-450.

Meier, W. N., Fetterer, F., Savoie, M., Mallory, S., Duerr, R., & Stroeve, J. (2017). NOAA/NSIDC climate data record of passive microwave sea ice concentration, version 3 [Computer software manual]. Boulder, Colorado USA. doi: https://doi.org/10.7265/N59P2ZTG

Parkinson, C. L. (2019). A 40-y record reveals gradual antarctic sea ice increases followed by decreases at rates far exceeding the rates seen in the arctic. *Proceedings of the National Academy of Sciences*, *116*(29), 14414–14423. doi: 10.1073/pnas.1906556116

Peng, G., Meier, W. N., Scott, D. J., & Savoie, M. H. (2013). A long-term and reproducible passive microwave sea ice concentration data record for climate studies and monitoring. *Earth System Science Data*, *5*(2), 311–318. doi: 10.5194/essd-5-311-2013

Polvani, L. M., & Smith, K. L. (2013). Can natural variability explain observed antarctic sea ice trends? new modeling evidence from CMIP5. *Geophysical Research Letters*, *40*(12), 3195-3199. doi: 10.1002/grl.50578

Raphael, M. N., & Hobbs, W. (2014). The influence of the large-scale atmospheric circulation on antarctic sea ice during ice advance and retreat seasons. *Geophysical Research Letters*, *41*, 5037-5045. doi: 10.1002/2014gl060365

Roach, L. A., Dean, S. M., & Renwick, J. A. (2018). Consistent biases in antarctic sea ice concentration simulated by climate models. *The Cryosphere*, *12*, 365-383.

Roach, L. A., Dörr, J., Holmes, C. R., Massonnet, F., Blockley, E. W., Notz, D., ... Bitz, C. M. (2020). Antarctic sea ice area in cmip6. *Geophysical Research Letters*, *47*(9), e2019GL086729. (e2019GL086729 10.1029/2019GL086729) doi: 10.1029/2019GL086729

Schlosser, E., Haumann, F. A., & Raphael, M. N. (2018). Atmospheric influences on the anomalous 2016 antarctic sea ice decay. *The Cryosphere*, *12*(3), 1103–1119. doi: 10.5194/tc-12-1103-2018

Shu, Q., Song, Z., & Qiao, F. (2015). Assessment of sea ice simulations in the CMIP5 models. *The Cryosphere*, *9*(1), 399–409. doi: 10.5194/tc-9-399-2015

Sigmond, M., & Fyfe, J. C. (2014). The antarctic sea ice response to the ozone hole in climate models. *Journal of Climate*, *27*(3), 1336-1342. doi: 10.1175/JCLI-D-13-00590.1

Simmonds, I. (2003). Modes of atmospheric variability over the southern ocean. *Journal of Geophysical Research: Oceans*, *108*(C4), SOV 5-1-SOV 5-30. doi: 10.1029/2000JC000542

Simmonds, I., & Keay, K. (2000, March). Mean Southern hemisphere extratropical cyclone behavior in the 40-year NCEP-NCAR reanalysis. *Journal of Climate*, *13*, 873-885. doi: 10.1175/1520-0442(2000)013⟨0873:MSHECB⟩2.0.CO;2

Simmonds, I., Rafter, A., Cowan, T., Watkins, A. B., & Keay, K. (2005, October). Large-scale Vertical Momentum, Kinetic Energy and Moisture Fluxes in the Antarctic Sea-ice Region. *Boundary-Layer Meteorology*, *117*(1), 149-177. doi: 10.1007/s10546-004-5939-6

Simpkins, G. R., Ciasto, L. M., & England, M. H. (2013). Observed variations in multidecadal antarctic sea ice trends during 1979–2012. *Geophysical Research*

Letters, *40*(14), 3643-3648. doi: 10.1002/grl.50715

Singh, H. K. A., Landrum, L., & Holland, M. M. (2020). *An overview of antarctic sea ice in the CESM2: Analysis of the seasonal cycle, predictability, and atmosphere-ocean-ice interactions.* (Manuscript submitted for publication to the *Journal of Advances in Modeling Earth Systems*)

Stammerjohn, S., Drinkwater, M. R., Smith, R. C., & Liu, X. (2003). Ice-atmosphere interactions during sea-ice advance and retreat in the western antarctic peninsula region. *Journal of Geophysical Research: Oceans*, *108*(C10). doi: 10.1029/2002JC001543

Stammerjohn, S., Massom, R., Rind, D., & Martinson, D. (2012). Regions of rapid sea ice change: An inter-hemispheric seasonal comparison. *Geophysical Research Letters*, *39*(6). doi: 10.1029/2012GL050874

Taschetto, A., Wainer, I., & Raphael, M. (2007). Interannual variability associated with semiannual oscillation in southern high latitudes. *Journal of Geophysical Research: Atmospheres*, *112*(D2). doi: 10.1029/2006JD007648

Turner, J., Bracegirdle, T. J., Phillips, T., Marshall, G. J., & Hosking, J. S. (2013). An initial assessment of antarctic sea ice extent in the CMIP5 models. *Journal of Climate*, *26*(5), 1473-1484. doi: 10.1175/JCLI-D-12-00068.1

van Den Broeke, M. (2000). The semi-annual oscillation and antarctic climate. part 4: a note on sea ice cover in the amundsen and bellingshausen seas. *International Journal of Climatology*, *20*(4), 455-462. doi: 10.1002/(SICI)1097-0088(20000330)20:4⟨455::AID-JOC482⟩3.0.CO;2-M

van Loon, H. (1967). The half-yearly oscillations in middle and high southern latitudes and the coreless winter. *Journal of the Atmospheric Sciences*, *24*(5), 472-486. doi: 10.1175/1520-0469(1967)024⟨0472:THYOIM⟩2.0.CO;2

van Loon, H., & Rogers, J. C. (1984). Interannual variations in the half-yearly cycle of pressure gradients and zonal wind at sea level on the southern hemisphere. *Tellus A*, *36A*(1), 76-86. doi: 10.1111/j.1600-0870.1984.tb00224.x

Wang, Z., Turner, J., Wu, Y., & Liu, C. (2019, 07). Rapid Decline of Total Antarctic Sea Ice Extent during 2014–16 Controlled by Wind-Driven Sea Ice Drift. *Journal of Climate*, *32*(17), 5381-5395. doi: 10.1175/JCLI-D-18-0635.1

Yuan, X., & Martinson, D. (2000, 05). Antarctic sea ice extent variability and its global connectivity*. *Journal of Climate*. doi: 10.1175/1520-0442(2000)013⟨1697:ASIEVA⟩2.0.CO;2

Yuan, X., & Martinson, D. G. (2001). The antarctic dipole and its predictability. *Geophysical Research Letters*, *28*(18), 3609-3612. doi: 10.1029/2001GL012969

Zunz, V., Goosse, H., & Massonnet, F. (2013). How does internal variability influence the ability of cmip5 models to reproduce the recent trend in southern ocean sea ice extent? *The Cryosphere*, *7*(2), 451–468. doi: 10.5194/tc-7-451-2013